

ON THE STRUCTURE OF THE 3D STRESS FIELD AND ITS 3D STRESS SINGULARITY
IN A 3D GRIFFITH CRACK

by

E. S. Folias

Department of Mathematics, University of Utah, Salt Lake City, UT 84112, USA

December 2006

Keywords: three-dimensional stress singularity, vertex singularity, three-dimensional corner singularity, surface cracks, three-dimensional Griffith crack, three-dimensional stress analysis

ABSTRACT

The author in this paper investigates the analytical three-dimensional stress field in the neighborhood of the intersection of a crack and a free surface. Utilizing the form of a general three-dimensional solution, which the author constructed in a previous paper, he recovers the explicit displacement and stress fields in this neighborhood. The analysis shows the stresses to be proportional to $\rho^{(-1/2-2\nu)}$.

The contents of this paper have recently been submitted for publication to the International Journal of Fracture, Dec. 1, 2012, however it was not considered for publication because of its submission form.

1. Introduction.

There exist in the literature a considerable number of papers which deal with the stress distribution, across the thickness of a cracked plate, both from an analytical as well as a numerical (FE) point of view. However, most of the existing analytical studies have focused on two dimensional considerations. This is because analytical solutions to the full three dimensional linear equations of elasticity are very difficult to obtain. On the other hand, three dimensional numerical studies generally require large amounts of computer resources, especially in certain critical areas where 3D cracks with corners may be present, in which areas they don't always give us the right answers. A relatively recent, but somewhat incomplete, historical discussion of the 3D Griffith crack problem, is given by Kown and Sun (2000).

Be that as it may, the effect that a specimen thickness has on the mechanism of failure, so far, is not very well understood. For example, the following questions may be raised

- (i) can a plate be characterized by a plane strain core sandwiched between two thin layers of plane stress at the surfaces ?
- (ii) do stress fields associated with long cracks have the same characteristics as those associated with short cracks, particularly in the vicinity of a free surface ?
- (iii) why is it that small cracks most often initiate at free surfaces, where they also propagate faster ?
- (iv) when is a plate classified as being thin or thick ?
- (v) what is the actual shape of deformation of the crack front immediately after the application of the load, and prior to the onset of fracture ?
- (vi) what is the strength of the stress singularity at the corner where the crack front intersects the free of stress surface of the plate ?
- (vii) does the order of the stress singularity have an effect on the shear lip formation ?
- (viii) and most importantly, what is the effect of the corner singularity on the fatigue life span of a structure, in the presence of surface cracks ?

Complete answers to the above, as well as other questions, have so far defied researchers, yet their answers are of great practical importance for the complete understanding of the phenomenon of 3D fracture. For example, the author in a previous paper (Folias and Wang, 1990), studied the 3D stress field of a plate weakened by the presence of a, through the thickness, hole, which he subsequently sharpened its numerical results even further by a more refined numerical analysis (see Fig. 1, Folias 1999), that provided a definite answer to the question (iv). More specifically, a plate with a hole is classified to be *thin* for ratios of radius to half thickness, (a/h) greater than 10, while it is classified to be *thick* for ratios of radius to half thickness (a/h) less than $1/10$. Moreover, he was able to show that most of the 3D effects are noticeable primarily in the region between $0.1 < (a/h) < 10$, where the stress concentration factor (at the center of the plate) is higher than the usual value of 3, a result predicted by a 2D theory. The result can be as high as 15-20 % larger, something that will have a substantial reduction on the fatigue life span of a structure by as much as 40 % or more, particularly in cases of bolt connections in bridges, airplane riveted connections or just plain holes. The practicing engineer,

therefore, must be cognizant of such 3D geometrical correction factors, if he is to guarantee the safety of a structure.

Moreover, in order to get a better understanding of what really happens at such corners, let us go back to the 2D problem of a circular hole, which is embedded into a plate and subjected to a remote tensile load σ_o (see Fig. 2). The local stresses at points A and B are given respectively by

$$\sigma_{\theta\theta}|_A = 3\sigma_o \quad ; \quad \sigma_{\theta\theta}|_B = -\sigma_o$$

suggesting that the material at point A is in a state of tension, while at point B it is in a state of compression. Next, let us consider the case where the radius of the hole becomes smaller and smaller, which suggests that point A approaches point B, closer and closer, and thus in the limit, it will form a jump in the stress profile ! As long as the radius of the hole is sufficiently large, the stresses induced by the remote load are all in the same plane of the applied load. However, if we examine the same condition but, within the theory of 3D, linear elasticity, and within the region where the hole meets the free surface of the plate, we see something totally different. Folias and Wang have shown (1990) that the displacement w is negative at point A, while positive at point B, thus creating locally a mode III stress profile (i.e. a tearing mode). Some skeptics may well suggest that this is the well known Poisson's effect. If that was the case, it would most likely be symmetric and not of a tearing mode type. This problem was studied by design in order to substantiate the presence of this tearing mode. The reader may also like to see more details in the paper (Folias, 1987). The same tearing mode has also been observed, experimentally, by Botsis and his students (2003 ?) in the similar case of a small diameter fiber, or cylindrical inclusion, meeting a free surface. The author was visiting the Lab at the time and was fortunate to be present during the execution of the experiment. For the case of a fiber, the reader may also like to see additional details in the paper (Folias, 1989). Thus, it becomes clear that making comparisons and extrapolations between 2D and 3D solutions based on physical intuition, at such neighborhoods, is not only difficult but also not advisable because of the boundary layer presence. Interestingly enough, based on some further numerical work carried out by the author for these type of problems, he was able to conclude that the region of influence of this boundary layer is restricted primarily to within approximately 10 % of the respective ratios of, hole radius to half thickness, or fiber radius to half thickness, or half crack length to half thickness in the case of a crack.

Returning back to our previous set of questions, in order for us to provide definite answers to questions (ii), (iii) and particularly (viii), we must know apriori the order of the stress singularity that prevails at such critical corners, where the crack front meets a free surface. It becomes *essential*, therefore, that we must determine its value.

It is costing the world billions and billions of dollars as a result of these type of failures, that almost always initiate at free surfaces and at such critical locations, needless to say the loss of so many lives. It is imperative, therefore, that a Fracture Community seeks an accurate and reliable *local surface fracture criterion*, which practicing engineers can use to guaranty the safety of a structure against catastrophic failures.

2. The general solution of a 3D Griffith crack.

Let us consider the equilibrium of a homogeneous, isotropic, and linear elastic, layer that occupies the space $|x| < \infty$, $|y| < \infty$, $|z| < h$ and which contains a finite, plane crack along its xz -plane (see Fig 3). The crack faces, defined by $|x| < c$, $y = \pm 0$, $|z| < h$, as well as the plate faces $|z| = h$, are assumed to be free of stress and constraint. The loading is assumed to be applied far away from the crack and along the outer periphery of the layer, i.e. along the boundaries $|x|, |y| \rightarrow \infty$.

In a previous paper (Folias, 1975), the author was able to derive a general 3D solution for the displacement and stress fields of the 3D Griffith crack. The solution was expressed in terms of Fourier Integrals and is valid throughout the region of the plate, including the corner points. From this general solution, he was then able to derive an asymptotic expansion in powers of $\eta = r / (h - z)$, which is applicable in the "inner layers" of the plate and all along the neighborhood of the crack front (see Folias 1975, eqs (90)-(98)). By expanding this asymptotic solution to also include higher orders of η , one then has, what the author refers to, as the "inner layers" solution, which is valid for all $z < h - \epsilon$, where ϵ is a very small quantity.

In the same paper, the author also ventured to derive an expression for the stress σ_{zz} , which was to be applicable to the "outer layers" of the plate and very very close to the free surface (see p. 670 of the above reference), by pushing the limit as z tends to h . Unfortunately, he was only able to express this limit in terms of Fourier integrals, but not explicitly.

In the present paper we will construct, based on the general solution, an asymptotic expansion which is to be valid within the region sector $\xi = (h - z) / r < 1$. While the inner expansion on the other hand, reflects the region sector $\xi = (h - z) / r > 1$. The two asymptotic expansions are then to be matched on the cone surface defined by $\xi = (h - z) / r = 1$. A cone surface that has its apex located at the corner of the crack and which it opens in the interior material of the plate.

What the author failed to recognize in 1975 was that this matching surface of the two asymptotic expansions was actually "slanted" rather than "parallel" to the free surface of the plate, something that he did not realize until the year of 2000.

3. Construction of the outer expansion in the neighborhood of the corner point.

The primary objective of the present analysis is to construct an asymptotic expansion that is to be valid within the immediate vicinity of the corner point and its adjacent free surface, i.e., the sector region $\xi = \frac{(h-z)}{r} < 1$ and all θ . Particular emphasis is to be placed on the order of the stress singularity that prevails at such corner regions. As it was previously noted, such information will be of great practical importance for it will help us obtain good estimates for the fatigue life span of a structure, in the presence of small surface cracks.

In order to accomplish this, we will be guided (i) by the general 3D solution, for the equilibrium of linear elastic layers, which the author constructed in a previous paper (Folias, 1975;

Folias, 1976) and which, he subsequently cast into a much more convenient form (Folias 1988a), and (ii) by the author's paper on the solution of the stress field at the intersection of a hole and a free surface (Folias, 1987). Thus, we may assume the *homogeneous displacement field* to be of the form, where $x, y, h-z$, and $r, h-z, \theta$ now reflect the local coordinates along the crack front :

(i) in rectangular cartesian coordinates :

$$\begin{aligned} u^{(h)} &= \frac{m}{m-2} \frac{\partial}{\partial x} (2\nu_o f + \Phi) + \frac{\partial g}{\partial y} \\ v^{(h)} &= \frac{m}{m-2} \frac{\partial}{\partial y} (2\nu_o f + \Phi) - \frac{\partial g}{\partial x} \\ w^{(h)} &= \frac{m}{m-2} \frac{\partial}{\partial z} (-2\nu_o f + \Phi) \end{aligned} \quad (1a) - (3a)$$

or

(ii) in cylindrical coordinates :

$$\begin{aligned} u_r^{(h)} &= \frac{m}{m-2} \frac{\partial}{\partial r} (2\nu_o f + \Phi) + \frac{1}{r} \frac{\partial g}{\partial \theta} \\ v_\theta^{(h)} &= \frac{m}{m-2} \frac{1}{r} \frac{\partial}{\partial \theta} (2\nu_o f + \Phi) - \frac{\partial g}{\partial r} \\ w^{(h)} &= \frac{m}{m-2} \frac{\partial}{\partial z} (-2\nu_o f + \Phi) \end{aligned} \quad (1b) - (3b)$$

where the functions f and g satisfy the 3D Laplace's equation, and

$$\nu_o = 1 - \nu, \quad m = \frac{1}{\nu}; \quad \text{and } f(r, (h-z), \theta), \quad g(r, (h-z), \theta) \quad (4)$$

$$\Phi = -(h-z) \frac{\partial f}{\partial z} . \quad (5)$$

To this, one may also add, if and when it is subsequently needed, the corresponding *particular solution* which, at this time for the sake of convenience, we chose to write in rectangular cartesian coordinates. The reason being that later, or in the future, one may have to use it in that form in order to deal with the boundary condition τ_{xy} , at $y = 0$:

$$u^{(p)} = \frac{\partial}{\partial x} \left\{ -\frac{\partial I_p}{\partial x} - y \frac{\partial I_q}{\partial y} - \frac{1}{m+1} z^2 \frac{\partial^2 I_q}{\partial x^2} \right\} \quad (6)$$

$$v^{(p)} = \frac{\partial}{\partial y} \left\{ \frac{4m}{m+1} I_q - \frac{\partial I_p}{\partial x} - y \frac{\partial I_q}{\partial y} - \frac{1}{m+1} z^2 \frac{\partial^2 I_q}{\partial x^2} \right\} \quad (7)$$

$$w^{(p)} = \frac{\partial}{\partial z} \left\{ \frac{1}{m+1} z^2 \frac{\partial^2 I_q}{\partial x^2} \right\} , \quad (8)$$

where in the above we have also adopted the additional definitions

$$\nu_o = 1 - \nu ; \quad \nu = \text{Poisson's ratio} \quad (9)$$

$$f = F \cos(a\theta) \quad (10)$$

$$g = G \sin(a\theta) \quad (11)$$

$$a = n + \frac{1}{2}, \quad n = 0, 1, 2, \dots \quad (12)$$

$$F = \frac{1}{\sqrt{r}} (r^2 + (h-z)^2)^{\nu_0} A_n \left\{ P_n^{2\nu_0} \left(i \frac{(h-z)}{r} \right) + P_n^{2\nu_0} \left(-i \frac{(h-z)}{r} \right) \right\} \quad (13)$$

$$G = \frac{1}{\sqrt{r}} (r^2 + (h-z)^2)^{\nu_0} B_n \left\{ P_n^{2\nu_0} \left(i \frac{(h-z)}{r} \right) + P_n^{2\nu_0} \left(-i \frac{(h-z)}{r} \right) \right\}. \quad (14)$$

Moreover, the coefficients A_n and B_n are constants which are to be determined from the remaining boundary conditions and where P stands for the Legendre's function. Additionally, the functions I_p , I_q are 2D solutions to Laplace's equation, i.e.

$$I_q = R_{[n]} r^{(n+\frac{1}{2})} \cos((n+\frac{1}{2})\theta), \quad n = 0, 1, 2, \dots \quad (15)$$

$$I_p = RR_{[n]} r^{(n+\frac{1}{2})} \cos((n+\frac{1}{2})\theta), \quad n = 0, 1, 2, \dots \quad (16)$$

Perhaps it is appropriate at this point to emphasize that, the functions f and g , by virtue of their construction, satisfy (i) Laplace's 3D equation, and (ii) their corresponding displacement functions satisfy also the 3D Navier's equations, as well as (iii) the free of stress boundary conditions on the plate face $z = h$. Thus, it remains for us to satisfy only the remaining boundary conditions on the plane $y = 0$.

4. The boundary conditions on the plane $y = 0$.

Without going into the mathematical details, the boundary conditions τ_{yz} and τ_{xy} , on the plane $y = 0$, or at $\theta = 0, \pi$, are automatically satisfied, provided the following two combinations vanish respectively

$$- \frac{2m}{m-2} \frac{1}{r} \frac{\partial \Phi}{\partial \theta} + \frac{\partial g}{\partial r} = 0 \quad (17)$$

$$2\nu_0 \frac{2m}{m-2} \frac{\partial}{\partial r} \left\{ \frac{1}{r} \frac{\partial f}{\partial \theta} \right\} - \frac{\partial^2 g}{\partial r^2} - \frac{\partial^2 g}{\partial z^2} = 0. \quad (18)$$

The reader may notice that in writing equation (18) we have omitted the $\tau_{xy}^{(p)}$ term. This is because these terms represent an expansion in ascending powers of \sqrt{r} which are to be taken care of by an alternate solution leading to a $(-1/2)$ order of stress singularity.

But, by virtue of its construction, our solution also satisfies the above equations all along that portion of the plane where $\theta = 0$ and $\xi < 1$, due to the presence of the factor $\sin(a\theta)$. Thus, one needs to satisfy equations (17)-(18) only along the remaining portion of the plane, where $\theta = \pi$ and $\xi < 1$.

Recalling next that $a = n + \frac{1}{2}$, $n = 0, 1, 2, \dots$, it is clear that our solution up to this point is valid for every value of n . Hence, by the principle of superposition, the sum of all of these solutions, from $n = 0$ to ∞ , is also a solution. This, therefore, provides us with two general functions, each of which leads to an infinite series. The unknown constant coefficients A_n and B_n , $n = 0, 1, 2, 3, 4, \dots$, are then to be determined, by satisfying the two conditions, i.e. eqs. (17)-(18), all along the plane sector $\theta = \pi$ and $\xi < 1$, in terms of the first two coefficients A_0, B_0 . In general, the constant coefficients will be functions of the material properties as well as of the external loading.

Next, each of the equations (17)-(18) may be written as an infinite series of the two variables ξ , and r , where

$$\xi = (h - z) / r. \quad (19)$$

5. Setting up the system.

Returning next to the functions f and g one has within the sector region $(h - z) < r$:

$$f = \frac{1}{\sqrt{r}} (r^2 + (h - z)^2)^{v_0} \sum_{n=0}^{\infty} A_n \{ P_n^{2v_0} (i \frac{(h-z)}{r}) + P_n^{2v_0} (-i \frac{(h-z)}{r}) \} \cos(a\theta) \quad (20)$$

$$g = \frac{1}{\sqrt{r}} (r^2 + (h - z)^2)^{v_0} \sum_{n=0}^{\infty} B_n \{ P_n^{2v_0} (i \frac{(h-z)}{r}) + P_n^{2v_0} (-i \frac{(h-z)}{r}) \} \sin(a\theta) \quad (21)$$

By direct substitution, the reader can easily show that the above asymptotic expansion satisfies (i) all the governing equations, and (ii) all the boundary conditions on the free surface $z = h$.

The above expansion should finally help to settle the question that was raised by Burton and Sinclair in 1984, whereby they misinterpreted the author's 1975 asymptotic expansion (Folias 1975) and erroneously concluded that his solution was not satisfying the boundary conditions on the free surface $|z| = h$!

In order for us to get a better insight and feel as to what these functions look like in terms of elementary functions, we will try next to simplify the first four terms of the above series expansion. Such information would be very helpful in making physical interpretations in the future

$$\begin{aligned} f = & \frac{1}{\sqrt{r}} (r^2 + (h - z)^2)^{v_0} \{ A_0 \cos(2v_0 \arctan(\frac{(h-z)}{r})) \cos(\frac{1}{2}\theta) + A_1 (\cos(2v_0 \arctan(\frac{(h-z)}{r}))) + \\ & + \frac{1}{2v_0} \frac{(h-z)}{r} \sin(2v_0 \arctan(\frac{(h-z)}{r})) \cos(\frac{3}{2}\theta) + \\ & + A_2 ((1 - \frac{3}{(4v_0^2-1)} \frac{(h-z)^2}{r^2}) \cos(2v_0 \arctan(\frac{(h-z)}{r})) + \frac{6v_0}{(4v_0^2-1)} \frac{(h-z)}{r} \sin(2v_0 \arctan(\frac{(h-z)}{r}))) \cos(\frac{5}{2}\theta) \} \\ & + A_3 ((8v_0^3 - 8v_0 - 30v_0 \frac{(h-z)^2}{r^2}) \cos(2v_0 \arctan(\frac{(h-z)}{r})) + (24v_0^2 - 9 - 15 \frac{(h-z)^2}{r^2}) \frac{(h-z)}{r} \\ & \sin(2v_0 \arctan(\frac{(h-z)}{r}))) \cos(\frac{7}{2}\theta) + \dots \} ; \quad (h - z) < r \end{aligned} \quad (22)$$

:

and

$$\begin{aligned}
g = & \frac{1}{\sqrt{r}} (r^2 + (h-z)^2)^{v_o} \{ B_0 \cos(2v_o \arctan(\frac{h-z}{r})) \sin(\frac{1}{2}\theta) + B_1 (\cos(2v_o \arctan(\frac{h-z}{r}))) + \\
& + \frac{1}{2v_o} \frac{(h-z)}{r} \sin(2v_o \arctan(\frac{h-z}{r})) \sin(\frac{3}{2}\theta) + \quad (23) \\
& + B_2 ((1 - \frac{3}{(4v_o^2-1)} \frac{(h-z)^2}{r^2}) \cos(2v_o \arctan(\frac{h-z}{r})) + \frac{6v_o}{(4v_o^2-1)} \frac{(h-z)}{r} \sin(2v_o \arctan(\frac{h-z}{r}))) \sin(\frac{5}{2}\theta) + \\
& + B_3 ((8v_o^3 - 8v_o - 30v_o \frac{(h-z)}{r}) \cos(2v_o \arctan(\frac{h-z}{r})) + (24v_o^2 - 9 - 158 \frac{(h-z)^2}{r^2}) \\
& \frac{(h-z)}{r} \sin(2v_o \arctan(\frac{h-z}{r}))) \sin(\frac{7}{2}\theta) + \dots \} ; \quad (h-z) < r
\end{aligned}$$

Utilizing spherical coordinates, it is interesting to see the alternate form of the function f which becomes

$$\begin{aligned}
f = & \frac{\rho^{2v_o-\frac{1}{2}}}{\sqrt{\cos(\phi)}} \cos(2v_o\phi) \{ A_0 \cos(\frac{1}{2}\theta) + A_1 [1 + \frac{1}{2v_o} \tan(\phi) \tan(2v_o\phi)] \cos(\frac{3}{2}\theta) + \quad (24) \\
& + A_2 [1 - \frac{3}{4b^2-1} \tan^2(\phi) + \frac{6b}{4b^2-1} \tan(\phi) \tan(2v_o\phi)] \cos(\frac{5}{2}\theta) + \dots \} ; \quad b = v_o ; \phi < \pi/4,
\end{aligned}$$

where ϕ now represents the angle from the free surface (see Fig. 4).

Similarly, the function g attains the same form except that the A 's now are replaced by B 's and the $\cos(\)$ terms are replaced by $\sin(\)$ terms. Naturally, transforming the expressions (22)-(23) from cylindrical coordinates to spherical coordinates does not represent a nouveau approach to this problem, but it simply provides us with some additional physical insight.

Returning next to the remaining boundary conditions, i.e., eqs. (17)-(18), one finds upon substituting the expressions ~~(22)~~-~~(23)~~ into the eqs, the unknown coefficients $A[n]$, $B[n]$ for $n = 0, \infty$ (see Appendix A, Maple print out). The first few coefficients of which, for a Poisson's ratio value of $\nu = 0.3$, are

$$\begin{aligned}
B[1] = & 1.123736260 B[0], \quad B[2] = 0.1354236058 B[0], \quad B[3] = -0.004092208002 B[0], \dots \\
A[1] = & 0.6000000012 A[0] + 2.283613918 B[0], \\
A[2] = & 0.2000000004 A[0] + 0.5789701630 B[0], \quad (25) \\
A[3] = & -0.01000400162 A[0] - 0.02723692495 B[0], \dots
\end{aligned}$$

The reader should notice that the magnitudes of these coefficients A_n , B_n decrease as n increases, a result which indicates that our numerical solution converges. Moreover, one may increase the number of coefficients, if a more accurate numerical result is desired, by taking into

account more powers of ξ . Hence, both the shear stresses τ_{yz} and τ_{xy} have also been shown to be satisfied, all along the plane $y = 0$ and $\xi < 1$, i.e. along the two sector planes

$$\theta = 0 \text{ and } \theta = \pi \text{ and within the sectors } 0 < \phi < \pi/4, \text{ or } 3\pi/4 < \phi < \pi. \quad (26)$$

The reader should be cautioned for the above asymptotic expansion is valid only along the cone sector $\xi = \frac{(h-z)}{r} < 1$, and that the actual matching between the two *inner* and *outer asymptotic expansions* takes place on the cone surface $\xi = 1$. The author, furthermore, believes that this cone surface is very close, if not on, to the tangent line which joins the corner crack point with the shear lip envelope point that lies on the plane $y = 0$.

Finally, the normal to the crack faces stress σ_{yy} also vanishes along the plane $\theta = \pi$, in view of the presence of the factor $\cos(\alpha\theta)$. Thus, the above represents a candidate solution, which solution, by direct substitution, can easily be shown to satisfy (i) all the governing equations, (ii) all the boundary conditions on the plate face $z = h$, and (iii) all the required boundary conditions on the plane $y = 0$ and $\xi < 1$. (For $\xi > 1$, the inner expansion (Folias 1975) was shown to satisfy the same boundary conditions for that region: see the following section). Consequently, the above represents, locally, a *candidate solution* which other researchers have missed. This suggests, therefore, that all other existing in the literature solutions are basically *incomplete*.

It may be emphasized here that Kawai (Kawai et. al., 1975; Smelser, 1979), even though he did not assume the *exact and natural local form* of the solution, he did also notice the presence of this singularity, but as he was increasing the number of equations in his truncated numerical system he began to experience severe convergence problems. Kawai, however, just like the author, did recognize the importance that, in the neighborhood of the corner point and its free surface, the exact and not the approximate satisfaction of the boundary conditions at $z = h$ was *essential*. This represents an important and subtle point of departure between his and other analyses presently available in the literature. Moreover, satisfying an integrated boundary condition is certainly not the same as satisfying the exact one, especially when it comes to such critical locations.

6. The asymptotic expansion in the inner layers.

On the other hand, along the remaining sector region, $y = 0$ and $\xi > 1$, the inner expansion was given in reference (Folias 1975), whereby the boundary conditions (17)-(18) were shown to be satisfied. Alternatively, one may also cast the inner expansion in the alternate form

$$\begin{aligned} f = & \frac{1}{\sqrt{r}} [r^2 + (h-z)^2]^{v_o} \{ [AA[0] \cos(2v_o \arctan(\frac{r}{(h-z)})) + BB[0] \sin(2v_o \arctan(\frac{r}{(h-z)}))] \cos(\frac{1}{2}\theta) \\ & + AA[1] [-\frac{3}{(2v_o-1)(2v_o+1)} \cos(2v_o \arctan(\frac{r}{(h-z)})) + \frac{3(h-z)}{2v_o(2v_o-1)(2v_o+1)r} \sin(2v_o \arctan(\frac{r}{(h-z)}))] \cos(\frac{3}{2}\theta) \\ & + BB[1] [\frac{(h-z)^2}{r((h-z)^2+r^2)^{1/2}}] [(2v_o(\frac{r}{(h-z)})^2+1) \cos((2v_o-1) \arctan(\frac{r}{(h-z)})) + \\ & + (2v_o-1) \sin((2v_o-1) \arctan(\frac{r}{(h-z)}))] \cos(\frac{3}{2}\theta) + \dots \} ; r < (h-z) \end{aligned} \quad (27)$$

:

however, additional terms of a similar nature may also need to be included.

Similarly, the function g has the same form except again that the $\cos(\)$ terms are replaced with $\sin(\)$ terms and the coefficients are different.

7. Matching the two asymptotic expansions.

As it was previously noted, the inner and outer asymptotic expansions are then to be matched on the cone surface $\xi = 1$ or $(h-z) = r$ and all θ . This matching, requires the continuity of both functions f and g , as well as their respective, normal to the cone surface, derivatives. The conditions then define the relationships that exist between the $AA[n]$ and the $A[n]$ coefficients, etc.

8. Discussion.

On a separate note, the form of the above *general but local to the surface, 3D, asymptotic solution, i.e.* (eqs (22)-(23)), may also be used to solve a whole class of problems involving dissimilar materials with different material angles and their interfaces which arise in the area of composite material systems, just like Williams (1952) so very well articulated in the 2D case of wedges. Such information is very much desirable for practical applications. What made the William's approach so powerful, was the fact that in his basic assumption

- (i) he had the *complete and natural form* of the solution that prevails at such, 2D, corner points
- (ii) the solution, in that neighborhood, was *separable* in the simple coordinate system which he considered

It is the essence of these two fundamental characteristics that the Williams' solution embraces that made his method so potentially attractive and functionally so powerful for the study of 2D material wedges.

Historically, general solutions of this type serve in a field as *superhighways*, that enable other researchers to use them and explore adjacent virgin areas of great practical interest and importance, areas that may have otherwise been previously inaccessible. An example of this is the well known general solution by Michell (see Timoshenko and Goodier, pp. 116-121). The William's (1952) asymptotic method of solution for the local stress field at the base of a material wedge angle is another example. Still another example, is the author's work for the method of solution of a cracked spherical shell (Folias, 1965a), as well as a cracked cylindrical shell (Folias, 1967). The development of the mathematical details of these two problems, allowed Folias (Fung ed. 1973) and his students to provide definite answers for the prediction of catastrophic failures in pressurized vessels. Additionally, other researchers, e.g. Sih (1977), Erdogan (see Sih 1977) and their students, utilizing the same mathematical steps, were able to make their own contributions and explore other related areas in pressurized vessels, as well as in, 2D, layered composite material systems weakened by the presence of cracks. The above represent only a few such

examples of superhighways in the field of fracture mechanics, yet there are many more scattered throughout the literature.

The potential benefits and impact that such superhighways have in the actual development and advancement of a field are enormous, yet they remain in the literature virtually unnoticed as insignificant contributions or as just simply being exercises in mathematics! This, the author believes, reflects a somewhat shortsighted point of view. The reality of the matter, however, is that mathematicians, in general, do not work on such topics. Only a different breed of engineers develop such superhighways, e.g. Bool () in electrical engineering who conceived the first basic steps of operational calculus. By attaching the stigma of *simply being studies in mathematics*, an engineering research community, perhaps inadvertently, may suppress and stifle progress in a field. Rarely does a *trial and error engineering* approach leads to an optimal safe structural design.

A perfect example of that was the design against catastrophic failures in pressurized vessels. Every time a researcher would change the value of one of the parameters in the problem the experimental results would lead to a different curve. Only an exact theory will take all these curves and collapse them onto one (see Folias, Fung ed. 1973). Another example was the work of Williams (1952), which provided us with definite answers for the prevention of wing type of failures in fighter aircraft. The author considers his work to be one of the most important contributions in design today. It is clear, therefore, that the use of *appropriate and relevant mathematics* in the study of physical engineering phenomena, almost always leads to much safer structural designs with an added economic advantage. Such studies are not just *exercises in mathematics*, but rather *exercises in smart and economic engineering designs of a different level*, and as such they should be encouraged.

Finally, it may be noted that the construction of the above solution was only possible because of the existence of the general 3D solution which the author previously developed (Folias, 1975 and Folias, 1988a), for the equilibrium of linear elastic layers. This general solution was based on the application of the Fourier Integral Transforms, an approach which was essential. More specifically, this general form of the solution revealed important and relevant characteristics that ultimately allowed the construction of the *natural form of the local solution, at such corner sectors*. This is precisely the reason why, in 1975, the author chose to use the FIT method of solution. Why? Because it makes no assumptions, whatsoever, of its behavior at such critical locations.

9. Conclusions.

Perhaps it is appropriate here to make a few general remarks and point out some important physical characteristics that our *candidate solution* possesses

- * all stresses $\sigma_{zz}, \tau_{xz}, \tau_{yz}$ do vanish on the plane $z = h$
- * the derivative of the stress σ_{zz} , with respect to z , also vanishes at $z = h$
- * all stresses are shown to be proportional to $\rho^{-1/2-2\nu}$

- * all displacements are shown to be proportional to $\rho^{1/2-2\nu}$
- * as the value of Poisson's ratio ν tends to zero, the square root stress singularity is recovered, which represents an exact solution
- * the author's observations on numerical results made in a previous paper (Folias 1988a, pp. 65-68) are substantiated
- * similar type of results, as those reported for the case of a hole, are also expected to prevail here too (Folias 1988b)
- * the results of the analysis suggest that, at the corner, the material can not sustain such high stresses and as a result the ninety degree corner must smooth out by rounding off first, before any relaxation, due to fracture, takes place
- * once the corner has been allowed to relax, by rounding of, then the crack will advance at the center of the plate thickness
- * the crack front resembles that of the cross sectional area of the heart of a sliced apple in half, whereby the crack front ' buckles if you will ' and tunnels its way into the middle section of the plate
- * finally, as one moves from $\phi = 0$ to $\phi = \pi / 4$, along the plane $\theta = 0$ (see Fig. 4) we see that for ratios of $(h-z) > r$ the function

$$f \sim 1 / \sqrt{r} (h-z)^{(2\nu_0)} \cdot \left\{ 1 + \frac{r^2}{(h-z)^2} \right\}^{\nu_0} \{A_0 \dots\} \quad (28)$$

which expression leads to the same asymptotic expansions reported by the author in his first paper (Folias 1975 , Folias 1976).

In conclusion, there is no stress relaxation, as far as the stress singularity is concerned, at such corner sectors. While it is true that, as one moves along the crack front and a little to the right, there is some stress relaxation in the functions of θ , ϕ , as one approaches the free surface, but this is due to the fact that the solution there must meet the free of stress boundary conditions. It is very much a similar effect as that of a concentrated line load acting on a half space (this problem was studied by Filon, see Timoshenko and Goodyear pp. 53-59), in which case the stresses have been shown to be proportional to

$$\sigma_{ij} \sim \left(\frac{1}{r}\right) \sin(\phi) , \quad (29)$$

where ϕ now represents the clockwise angle from the free surface. The reader may easily examine the various limits, example as r tends to zero or as ϕ tends to zero, a condition that reflects a limit of the form $\infty \times 0$. Clearly, the limit depends on the path of approach.

Similarly, in the vicinity of the corner point and close to the free surface, the shear stresses τ_{xz} and τ_{yz} must vanish at $z = h$ in order to satisfy the boundary conditions. Thus their behavior there is of the form

$$\tau \sim \rho^{(-\frac{1}{2}-2\nu)} \sin(\phi) \dots \quad (30)$$

which attains different limits, as one approaches the corner point along different paths. (for more details, see comments made by the author pp. 65-68, Folias 1988a and its connection to Filon's problem Timmoshenko and Goodier 1987).

Finally, along the free surface and along the crack prolongation $\theta = 0$, the normal to the crack faces stress σ_{yy} , for a Poisson's ratio of 0.3 becomes :

$$\sigma_{yy} = -\{8.0176 A_0 + 35.4515 B_0\} \rho^{-1.1} ; \theta = 0, \phi = 0 \quad (31)$$

where the coefficients A_0 and B_0 are proportionally to $(-\sigma_o)$.

On a practical note, the author in a previous paper has shown (Folias et. al. 1990) that in the case of a plate with a hole and for ratios of $(a/h) > 0.5$ a crack is most likely to initiate in the middle section of the plate, while for ratios of $(a/h) < 0.5$ a crack is most likely to initiate close to the free surface. Such information is of great practical importance in the design of high performance aircraft (rivets or connections), or in rivets of aging aircraft or in structural connections for bridges, etc. It is now possible and relatively easy to derive a reliable *fatigue growth criterion* for the lifespan prediction of a structure, in the presence of small surface flaws. Such type of failures have been shown to be even more pronounced when lateral vibrations, and or high temperatures, are present (see Folias 1968; Do and Folias, 1971). For the novice in the field of Fracture, such a criterion usually requires two type of ingredients (i) the type of stress analysis provided above (which reflects a 95% of the total effort) and (ii) an energy balance and or a fatigue growth analysis (which reflects another 5% of the total effort).

In studying the later, the author would like to acknowledge the work of G. Sih (Fracture Vol. I), who in a very clever way utilized Claperon's theorem to show how the strain energy of a cracked material system can be evaluated in a very simple and very effective way, by knowing only the crack opening displacement. The author has long considered this to be one of the most important and major contributions in the field of Fracture. Perhaps the reader may also like to reflect on the fact that, if it was not for the existence of the work of Inglis (1913), the Griffith Fracture criterion perhaps may not exist! Yet, very few researchers are even aware of Inglis's work!

It is costing the world billions and billions of dollars, as a result of these type of failures, that almost always initiate at free surfaces and at such critical locations, needless to say the loss of so many lives. It is imperative, therefore, that the world Fracture Community develops a reliable and accurate *fracture criterion for the prediction of the fatigue growth of surface cracks*, that *practicing engineers* may use to guaranty the safety of a structure, against catastrophic failures.

Although this has been the author's *primary objective* in his big picture, as he embarked in his 3D work, the political games played, however, have been horrendous ! But, can we afford not to pursue every angle that may lead us to safer engineering designs ?

Finally, the question of infinite displacements has been addressed by Wilcox (1979), at the request of the author. The mere fact that for certain Poisson's ratios, $\nu > 1/4$, the displacements are singular at such corner points this does not imply that one may not be able to extract useful and practical information from the solution. The 2D solution is a perfect example of that. Although the stress field in 2D is singular at the crack tip, the well known *2D fracture criterion* provides us with very good results for the safety of engineering structures, as long as there are no small surface cracks present. At such critical locations, the fatigue growth characteristics of small cracks are very much different and as such engineering designers must include an *appropriate local geometrical correction factor* to account for that.

10. Construction of a second solution in the neighborhood of the corner point :

In a similar manner, one has for a second solution within the sector $\xi < 1$, the following

$$FF = \frac{1}{\sqrt{r}} (r^2 + (h-z)^2)^{\nu_0} AAA_n \left\{ Q_n^{2\nu_0} \left(i \frac{(h-z)}{r} \right) + Q_n^{2\nu_0} \left(-i \frac{(h-z)}{r} \right) \right\} \quad (36)$$

$$GG = \frac{1}{\sqrt{r}} (r^2 + (h-z)^2)^{\nu_0} BBB_n \left\{ Q_n^{2\nu_0} \left(i \frac{(h-z)}{r} \right) + Q_n^{2\nu_0} \left(-i \frac{(h-z)}{z} \right) \right\} . \quad (37)$$

The above, therefore, represents another candidate solution which, in the event that it is not linearly independent from the previous one, then requires the presence of a logarithmic term. In such a case, the reader is referred to Wyllie (1975), for the standard procedure in recovering the solution.

Additionally, the $(-1/2)$ order of stress singularity is also another candidate solution which can be obtained by a similar type of analysis. However, only the highest order is relevant and of any practical value.

Finally, a remark is in order regarding the special case when Poisson's ratio reaches the special value of $\nu = 1/4$, in which case the stresses are proportional

$$\sigma_{ij} \sim \rho^{-1} , \quad (38)$$

a result which suggests that the displacements now are proportionally to $\ln(\rho)$. In such case, one must differentiate the solution with respect to the parameter ν , and then take the limit as $\nu \rightarrow 1/4$ (see Wyllie 1975 pp. 388-393), which then recovers the desired logarithmic term.

ACKNOWLEDGMENT

The author would like to acknowledge and thank Professor Cal Wilcox for taking the time to prove (i) the 3D uniqueness theorem and (ii) the completeness of the author's 3D eigenfunctions (Folias, 1975).

The Fracture Community owes a debt of gratitude to Professor Wilcox for his *enormous, significant and lasting* contributions to the field of Fracture Mechanics.

Professor Wilcox, who in his career was first a *physicist*, second an *applied* mathematician, and third a *pure* mathematician, not only had the necessary physical background but he also had the required mathematical skills to complete such a uniqueness proof.

REFERENCES.

- W. Kown and C.T. Sun, *International Journal of Fracture*, 104 (2000), pp. 291-315.
- E. S. Folias and J. J. Wang, " On the Three-Dimensional Stress Field around a Circular Hole in a Plate of Arbitrary Thickness " *Computational Mechanics* 6 (1990) pp. 379-391.
- E. S. Folias, " Failure Correlation Between Pressurized Vessels and Plates " *International Journal of Pressure Vessels and Piping*, 76 (1999) pp. 803-811.
- E. S. Folias, On the Three-Dimensional Theory of Cracked Plates, *Journal of Applied Mechanics* 7 (1975), pp. 245-254.
- E. S. Folias, " Closure to the Discussion on 'Discussion on the Three-Dimensional Theory of Cracked Plates " , *Journal of Applied Mechanics* 43 (1976), pp. 374-375.
- E. S. Folias, On the stress singularities at the intersection of a cylindrical inclusion with the free surface of a plate, *International Journal of Fracture* , 39 : 1989, pp. 25-34.
- E. S. Folias, "The 3D Stress Field at the Intersection of a Hole and a Free Surface " , *International Journal of Fracture* 35 (1987), pp. 187-194.
- T. Kawai, Y. Fujitani, On the singular solutions of three-dimensional crack problems, presented at the Second International Conference on Mechanical Behavior of Materials, Boston, MA Aug. 16-20, 1975.
- Smelser, Ron, 1979, Summary of Discussion of T. Kawai and E. S. Folias, March 1979, University of Pittsburgh, Private communication
- E. S. Folias, " Some Remarks on Three Dimensional Fracture " *ASTM STP 969 Publication, Fracture Mechanics 19th Symposium*, edited by T. A. Cruse (1988a), pp. 56-72.
- E. S. Folias, " Recent Advances on 3D Elasticity Problems Related to Fracture " , *ASME AMD-Vol 91: Analytical, Numerical, and Experimental Aspects of Three Dimensional Fracture Processes*, edited by A. Rosakis, K. Ravi-Chandar, & Y. Rajapakse (1988b), pp. 267-277.
- S. Timoshenko & J. Goodier, *Theory of Elasticity* , 1987 McGraw-Hill, pp. 53-59.
- R. Wyllie, *Advanced Engineering Mathematics*, 1975 McGraw-Hill, pp. 388-393.
- M. L. Williams, *Journal of Applied Mechanics*, 19 (1952) 526-530; 24 (1957)
- E. S. Folias, The stresses in a cracked spherical shell, *Journal of Mathematics and Physics* XLIV 1965a, pp. 164-176.

E. S. Folias, An axial crack in a pressurized cylindrical shell, International Journal of Fracture 3, 1967, pp. 104-113.

E. S. Folias, On the steady-state transverse vibrations of a cracked plate, Engineering Fracture Mechanics Journal, 1 (1968) pp. 363-368.

S. H. Do and E. S. Folias, On the steady-state transverse vibrations of a cracked spherical shell, International Journal of Fracture 7 (1971) pp. 23-37.

C. H. Wilcox, Uniqueness Theorems for Displacement Fields with Locally Finite Energy in Linear Elastostatics, Journal of Elasticity, Vol. 9, No. 3, July 1979, pp. 221-243.

C. H. Wilcox, Completeness of the Eigenfunctions for Griffith Cracks in Plates of Finite Thickness, UTEC CE 79-024, Dec.. 1978.

G. C. Sih, Plates and Shells with Cracks, Mechanics of Fracture 3, edited G. Sih 1977.

G. C. Sih, Fracture Vol. I

W. S. Burton and G. S. Sinclair , IJF vol. 25, 1984, pp. 3-33.

C. E. Inglis, Stresses in a plate due to the presence of cracks and sharp corners, Trans. Instn. Naval Architects LV(1), 219, 1913.

> # APPENDIX A #

> restart:

> b := vσ;

$$b := v\sigma \quad (1)$$

> xi := $\frac{(h-z)}{r}$;

$$\xi := \frac{h-z}{r} \quad (2)$$

> # THE FIRST FEW COEFFICIENTS #

> B₃ := factor($\frac{1}{40} ((256 v\sigma^5 - 1024 v\sigma^4 + 3168 v\sigma^3 - 5408 v\sigma^2 + 4409 v\sigma - 1890) B_0) / ((v\sigma + 1) (256 v\sigma^6 - 1280 v\sigma^5 + 4192 v\sigma^4 - 10112 v\sigma^3 + 12889 v\sigma^2 - 9659 v\sigma + 6018) v\sigma)$);

$$B_3 := \frac{1}{40} ((256 v\sigma^5 - 1024 v\sigma^4 + 3168 v\sigma^3 - 5408 v\sigma^2 + 4409 v\sigma - 1890) B_0) / ((v\sigma + 1) (256 v\sigma^6 - 1280 v\sigma^5 + 4192 v\sigma^4 - 10112 v\sigma^3 + 12889 v\sigma^2 - 9659 v\sigma + 6018) v\sigma) \quad (3)$$

> B₂

:= factor($(B_0 (256 v\sigma^6 - 1280 v\sigma^5 + 4192 v\sigma^4 - 9344 v\sigma^3 + 11353 v\sigma^2 - 7979 v\sigma + 2802)) / (256 v\sigma^6 - 1280 v\sigma^5 + 4192 v\sigma^4 - 10112 v\sigma^3 + 12889 v\sigma^2 - 9659 v\sigma + 6018)$);

$$B_2 := \frac{B_0 (v\sigma - 1) (v\sigma - 2) (256 v\sigma^4 - 512 v\sigma^3 + 2144 v\sigma^2 - 1888 v\sigma + 1401)}{256 v\sigma^6 - 1280 v\sigma^5 + 4192 v\sigma^4 - 10112 v\sigma^3 + 12889 v\sigma^2 - 9659 v\sigma + 6018} \quad (4)$$

> B₁

:= factor($\frac{9}{5} ((256 v\sigma^6 - 1280 v\sigma^5 + 4192 v\sigma^4 - 9856 v\sigma^3 + 12377 v\sigma^2 - 9099 v\sigma + 4690) B_0) / (256 v\sigma^6 - 1280 v\sigma^5 + 4192 v\sigma^4 - 10112 v\sigma^3 + 12889 v\sigma^2 - 9659 v\sigma + 6018)$);

$$B_1 := \frac{9}{5} ((256 v\sigma^6 - 1280 v\sigma^5 + 4192 v\sigma^4 - 9856 v\sigma^3 + 12377 v\sigma^2 - 9099 v\sigma + 4690) B_0) / (256 v\sigma^6 - 1280 v\sigma^5 + 4192 v\sigma^4 - 10112 v\sigma^3 + 12889 v\sigma^2 - 9659 v\sigma + 6018) \quad (5)$$

$$+ 4690) B_0) / (256 v o^6 - 1280 v o^5 + 4192 v o^4 - 10112 v o^3 + 12889 v o^2 - 9659 v o + 6018)$$

$$\begin{aligned} > A_3 := \frac{1}{280} (1024 m v o^8 A_0 - 5888 m v o^7 A_0 + 20608 m v o^6 A_0 - 3072 m v o^6 B_0 \\ & - 53024 m v o^5 A_0 + 9216 m v o^5 B_0 + 6144 v o^6 B_0 + 81892 m v o^4 A_0 \\ & - 21120 m v o^4 B_0 - 18432 v o^5 B_0 - 77303 m v o^3 A_0 + 36096 m v o^3 B_0 \\ & + 42240 v o^4 B_0 + 53049 m v o^2 A_0 - 25164 m v o^2 B_0 - 72192 v o^3 B_0 \\ & - 18054 m v o A_0 + 8076 m v o B_0 + 50328 v o^2 B_0 - 4608 m B_0 - 16152 v o B_0 \\ & + 9216 B_0) / (m v o^2 (256 v o^6 - 1280 v o^5 + 4192 v o^4 - 10112 v o^3 + 12889 v o^2 \\ & - 9659 v o + 6018) (4 v o - 3) (v o^2 - 1)) \end{aligned}$$

$$\begin{aligned} A_3 := \frac{1}{280} (1024 m v o^8 A_0 - 5888 m v o^7 A_0 + 20608 m v o^6 A_0 - 3072 m v o^6 B_0 \\ - 53024 m v o^5 A_0 + 9216 m v o^5 B_0 + 6144 v o^6 B_0 + 81892 m v o^4 A_0 \\ - 21120 m v o^4 B_0 - 18432 v o^5 B_0 - 77303 m v o^3 A_0 + 36096 m v o^3 B_0 \\ + 42240 v o^4 B_0 + 53049 m v o^2 A_0 - 25164 m v o^2 B_0 - 72192 v o^3 B_0 \\ - 18054 m v o A_0 + 8076 m v o B_0 + 50328 v o^2 B_0 - 4608 m B_0 - 16152 v o B_0 \\ + 9216 B_0) / (m v o^2 (256 v o^6 - 1280 v o^5 + 4192 v o^4 - 10112 v o^3 + 12889 v o^2 \\ - 9659 v o + 6018) (4 v o - 3) (v o^2 - 1)) \end{aligned} \quad (6)$$

$$\begin{aligned} > A_2 := \frac{1}{5} (1024 m v o^8 A_0 - 5888 m v o^7 A_0 + 20608 m v o^6 A_0 - 1536 m v o^6 B_0 \\ - 53024 m v o^5 A_0 + 4608 m v o^5 B_0 + 3072 v o^6 B_0 + 81892 m v o^4 A_0 \\ - 10560 m v o^4 B_0 - 9216 v o^5 B_0 - 77303 m v o^3 A_0 + 22656 m v o^3 B_0 \\ + 21120 v o^4 B_0 + 53049 m v o^2 A_0 - 17190 m v o^2 B_0 - 45312 v o^3 B_0 \\ - 18054 m v o A_0 + 6054 m v o B_0 + 34380 v o^2 B_0 - 4608 m B_0 - 12108 v o B_0 \\ + 9216 B_0) / ((4 v o - 3) (256 v o^6 - 1280 v o^5 + 4192 v o^4 - 10112 v o^3 \\ + 12889 v o^2 - 9659 v o + 6018) v o m); \end{aligned}$$

$$\begin{aligned} A_2 := \frac{1}{5} (1024 m v o^8 A_0 - 5888 m v o^7 A_0 + 20608 m v o^6 A_0 - 1536 m v o^6 B_0 \\ - 53024 m v o^5 A_0 + 4608 m v o^5 B_0 + 3072 v o^6 B_0 + 81892 m v o^4 A_0 \\ - 10560 m v o^4 B_0 - 9216 v o^5 B_0 - 77303 m v o^3 A_0 + 22656 m v o^3 B_0 \\ + 21120 v o^4 B_0 + 53049 m v o^2 A_0 - 17190 m v o^2 B_0 - 45312 v o^3 B_0 \\ - 18054 m v o A_0 + 6054 m v o B_0 + 34380 v o^2 B_0 - 4608 m B_0 - 12108 v o B_0 \\ + 9216 B_0) / ((4 v o - 3) (256 v o^6 - 1280 v o^5 + 4192 v o^4 - 10112 v o^3 \end{aligned} \quad (7)$$

$$+ 12889 v o^2 - 9659 v o + 6018) v o m)$$

$$\begin{aligned} > A_1 := \frac{3}{5} (1024 m v o^8 A_0 - 5888 m v o^7 A_0 + 20608 m v o^6 A_0 - 512 m v o^6 B_0 \\ & - 53024 m v o^5 A_0 + 1536 m v o^5 B_0 + 1024 v o^6 B_0 + 81892 m v o^4 A_0 \\ & - 3520 m v o^4 B_0 - 3072 v o^5 B_0 - 77303 m v o^3 A_0 + 8576 m v o^3 B_0 + 7040 v o^4 B_0 \\ & + 53049 m v o^2 A_0 - 6754 m v o^2 B_0 - 17152 v o^3 B_0 - 18054 m v o A_0 \\ & + 2466 m v o B_0 + 13508 v o^2 B_0 - 4608 m B_0 - 4932 v o B_0 + 9216 B_0) / ((4 v o \\ & - 3) (256 v o^6 - 1280 v o^5 + 4192 v o^4 - 10112 v o^3 + 12889 v o^2 - 9659 v o \\ & + 6018) v o m); \end{aligned}$$

$$\begin{aligned} A_1 := \frac{3}{5} (1024 m v o^8 A_0 - 5888 m v o^7 A_0 + 20608 m v o^6 A_0 - 512 m v o^6 B_0 \\ - 53024 m v o^5 A_0 + 1536 m v o^5 B_0 + 1024 v o^6 B_0 + 81892 m v o^4 A_0 \\ - 3520 m v o^4 B_0 - 3072 v o^5 B_0 - 77303 m v o^3 A_0 + 8576 m v o^3 B_0 \\ + 7040 v o^4 B_0 + 53049 m v o^2 A_0 - 6754 m v o^2 B_0 - 17152 v o^3 B_0 \\ - 18054 m v o A_0 + 2466 m v o B_0 + 13508 v o^2 B_0 - 4608 m B_0 - 4932 v o B_0 \\ + 9216 B_0) / ((4 v o - 3) (256 v o^6 - 1280 v o^5 + 4192 v o^4 - 10112 v o^3 \\ + 12889 v o^2 - 9659 v o + 6018) v o m) \end{aligned} \quad (8)$$

THE FUNCTIONS

$$\begin{aligned} > f := \frac{(r^2 + (h-z)^2)^b}{r^{(\frac{1}{2})}} \cdot \left(A[0] \cdot \cos(2 \cdot b \cdot \arctan(xi)) \cdot \cos\left(\frac{1}{2} \cdot \theta\right) + A[1] \cdot \left(\cos(2 \cdot b \right. \right. \\ & \cdot \arctan(xi)) + \frac{1}{2 \cdot b} \cdot xi \cdot \sin(2 \cdot b \cdot \arctan(xi)) \left. \right) \cdot \cos\left(\frac{3}{2} \cdot \theta\right) + A[2] \cdot \left(\left(1 \right. \right. \\ & \left. \left. - \frac{3}{4 \cdot b^2 - 1} \cdot \xi^2 \right) \cdot \cos(2 \cdot b \cdot \arctan(xi)) + \frac{6 \cdot b}{4 \cdot b^2 - 1} \cdot xi \cdot \sin(2 \cdot b \cdot \arctan(xi)) \right) \\ & \cdot \cos\left(\frac{5}{2} \cdot \theta\right) + A[3] \cdot \left((-30 \cdot b \cdot \xi^2 - 8 \cdot b + 8 \cdot b^3) \cdot \cos(2 \cdot b \cdot \arctan(xi)) + (-15 \right. \\ & \left. \cdot \xi^2 + 24 \cdot b^2 - 9) \cdot xi \cdot \sin(2 \cdot b \cdot \arctan(xi)) \right) \cdot \cos\left(\frac{7}{2} \cdot \theta\right) \left. \right): \end{aligned}$$

$$\begin{aligned} > EQ := \text{simplify}\left(\text{diff}(f, r, r) + \frac{1}{r} \cdot \text{diff}(f, r) + \frac{1}{r^2} \cdot \text{diff}(f, \theta, \theta) + \text{diff}(f, z, \right. \\ & \left. z) \right): \end{aligned}$$

$$\begin{aligned} > g := \frac{(r^2 + (h-z)^2)^b}{r^{(\frac{1}{2})}} \cdot \left(B[0] \cdot \cos(2 \cdot b \cdot \arctan(xi)) \cdot \sin\left(\frac{1}{2} \cdot \theta\right) + B[1] \cdot \left(\cos(2 \cdot b \right. \right. \\ & \left. \left. \arctan(xi)) + \frac{1}{2 \cdot b} \cdot xi \cdot \sin(2 \cdot b \cdot \arctan(xi)) \right) \cdot \sin\left(\frac{3}{2} \cdot \theta\right) + B[2] \cdot \left(\left(1 \right. \right. \\ & \left. \left. - \frac{3}{4 \cdot b^2 - 1} \cdot \xi^2 \right) \cdot \cos(2 \cdot b \cdot \arctan(xi)) + \frac{6 \cdot b}{4 \cdot b^2 - 1} \cdot xi \cdot \sin(2 \cdot b \cdot \arctan(xi)) \right) \\ & \cdot \sin\left(\frac{5}{2} \cdot \theta\right) + B[3] \cdot \left((-30 \cdot b \cdot \xi^2 - 8 \cdot b + 8 \cdot b^3) \cdot \cos(2 \cdot b \cdot \arctan(xi)) + (-15 \right. \\ & \left. \cdot \xi^2 + 24 \cdot b^2 - 9) \cdot xi \cdot \sin(2 \cdot b \cdot \arctan(xi)) \right) \cdot \sin\left(\frac{7}{2} \cdot \theta\right) \left. \right): \end{aligned}$$

$$\begin{aligned} & \cdot \arctan(\xi) + \frac{1}{2 \cdot b} \cdot \xi \cdot \sin(2 \cdot b \cdot \arctan(\xi)) \Big) \cdot \sin\left(\frac{3}{2} \cdot \theta\right) + B[2] \cdot \left(\left(1 \right. \right. \\ & \left. \left. - \frac{3}{4 \cdot b^2 - 1} \cdot \xi^2 \right) \cdot \cos(2 \cdot b \cdot \arctan(\xi)) + \frac{6 \cdot b}{4 \cdot b^2 - 1} \cdot \xi \cdot \sin(2 \cdot b \cdot \arctan(\xi)) \right) \\ & \cdot \sin\left(\frac{5}{2} \cdot \theta\right) + B[3] \cdot \left((-30 \cdot b \cdot \xi^2 - 8 \cdot b + 8 \cdot b^3) \cdot \cos(2 \cdot b \cdot \arctan(\xi)) + (-15 \cdot \xi^2 \right. \\ & \left. + 24 \cdot b^2 - 9) \cdot \xi \cdot \sin(2 \cdot b \cdot \arctan(\xi)) \right) \cdot \sin\left(\frac{7}{2} \cdot \theta\right) \Big) : \end{aligned}$$

> $ft := \text{diff}(f, \theta) :$

> $ftp := \text{eval}(\text{subs}(\theta = \text{Pi}, ft)) :$

> $gp := \text{eval}(\text{subs}(\theta = \text{Pi}, g)) :$

> $PHtp := -(h - z) \cdot \text{diff}(ftp, z) :$

>

>

> # THE BOUNDARY CONDITIONS ALONG THE SECTOR $y=0$ AND $\xi < 1$ #

>

> $EQ1 := -\frac{2 \cdot m}{(m - 2)} \cdot \frac{PHtp}{r} + \text{diff}(gp, r) :$

> $\text{subs}\left(\frac{(h - z)}{r} = x, \%\right) :$

> $\text{subs}((h - z) = r \cdot x, \%) :$

> $\text{subs}((-2 \cdot h + 2 \cdot z) = -2 \cdot r \cdot x, \%) :$

> $\text{factor}(\%) :$

> $Q1 := \text{simplify}\left(\left(\frac{4 \cdot r^{\frac{3}{2}} \cdot (m - 2) \cdot (1 + x^2) \cdot vo \cdot (2 \cdot vo - 1) \cdot (2 \cdot vo + 1) \cdot \%}{(r^2 \cdot (1 + x^2))^{vo}}\right)\right) :$

> $QQ1 := \text{series}(Q1, x, 10) :$

> $\text{eval}(\text{subs}(x = 0, QQ1)) ;$

0

(9)

>

> $\text{simplify}(\text{coeff}(QQ1, x^2)) ;$

0

(10)

>

> $\text{simplify}(\text{coeff}(QQ1, x^4)) ;$

0

(11)

> # ETC #

>

>

>

> $EQ2 := \frac{2 \cdot vo \cdot 2 \cdot m}{(m - 2)} \cdot \text{diff}\left(\frac{ftp}{r}, r\right) - \text{diff}(gp, r, r) - \text{diff}(gp, z, z) :$

```

> subs( (h-z)/r = x, % ) :
> subs( (h-z) = r*x, % ) :
> subs( (-2*h+2*z) = -2*r*x, % ) :
>
> factor( % ) :
> Q2 := 1 / (vo*(vo+1) - 1) * (simplify( (32 / (r^2*(1+x^2)))^vo * r^(5/2) * (vo-1)*(vo+1)*(4*vo
- 5)*(m-2)*(4*vo-9)*(2*vo-1)*(2*vo+1)*vo*(1+x^2)*(vo^2-1) ) * 1 ) :
> QQ2 := series(Q2, x, 10) :
> subs(x=0, QQ2);
0 (12)
>
> simplify(coeff(QQ2, x^2));
0 (13)
>
> simplify(coeff(QQ2, x^4));
0 (14)
>
> # ETC #
>
> # EXAMPLE : THE NUMERICAL VALUE OF THE COEFFICIENTS FOR POISSON'S
RATIO OF 0.3 IS GIVEN BELOW #
>
> vo := 0.7; m := 1/0.3;
vo:= 0.7
m:= 3.333333333 (15)
> evalf(B[1]);
1.123736260 B0 (16)
> evalf(B[2]);
0.1354236058 B0 (17)
> evalf(B[3]);
-0.004092208002 B0 (18)
>
> # ETC #
>
> evalf(A[1]);
(19)

```

$$0.6000000012 A_0 + 2.283613918 B_0 \quad (19)$$

> evalf(A[2]);

$$0.2000000004 A_0 + 0.5789701630 B_0 \quad (20)$$

> evalf(A[3]);

$$-0.01000400162 A_0 - 0.02723692495 B_0 \quad (21)$$

> # ETC #

> # CONCLUSION : THE VALUE OF THE COEFFICIENTS $A[n]$ AND $B[n]$ DO
DECREASE AS n INCREASES , SUGGESTING CONVERGENCE #

> # REMARK : IN THE EVENT THAT ONE IS INTERESTED IN EXTENDING THE
SERIES TO SAY UP TO COEFFS $A[10]$ AND $B[10]$, THEN THE SHEAR
STRESSES WILL BE SATISFIED UP TO ORDER $(x^2)^{10}$
RESPECTIVELY AND SO ON ... #

APPENDIX B

A POINT OF CLARIFICATION :

The main goal of the above paper was to show only what the prevailing strength of the stress singularity is, at such corners. As a result, eqs. (20)-(21) reflect only the first term of many others of a similar nature. The reader, however, should realize that up to this point of the analysis the parameter $b = \nu_o$ is still largely arbitrary. Consequently, the general form of the function f is :

$$f = \frac{1}{\sqrt{r}} \sum_{n=0}^{\infty} \sum_{k=0}^{\infty} A_{[n,k]} [r^2 + (h-z)^2]^{(b+k/2)} \{P_n^{2b+k}(I \frac{(h-z)}{r}) + P_n^{2b+k}(-I \frac{(h-z)}{r})\} \cos(a\theta) ,$$

which for $k=0$ reduces to eq. (20). But, for purposes of showing what the order of the stress singularity is, one really needs to consider only the first term.

Similarly, the general form of the inner expansion of the solution may be written in the form :

$$f = \frac{1}{\sqrt{r}} \sum_{n=0}^{\infty} AA[n] (h-z)^{2b} (\frac{r}{(h-z)})^{a+\frac{1}{2}} {}_2F_1(-b + \frac{3}{4} + \frac{1}{2}a, -b + \frac{1}{4} + \frac{1}{2}a, 1+a, -\frac{r^2}{(h-z)^2}) \cos(a\theta).$$

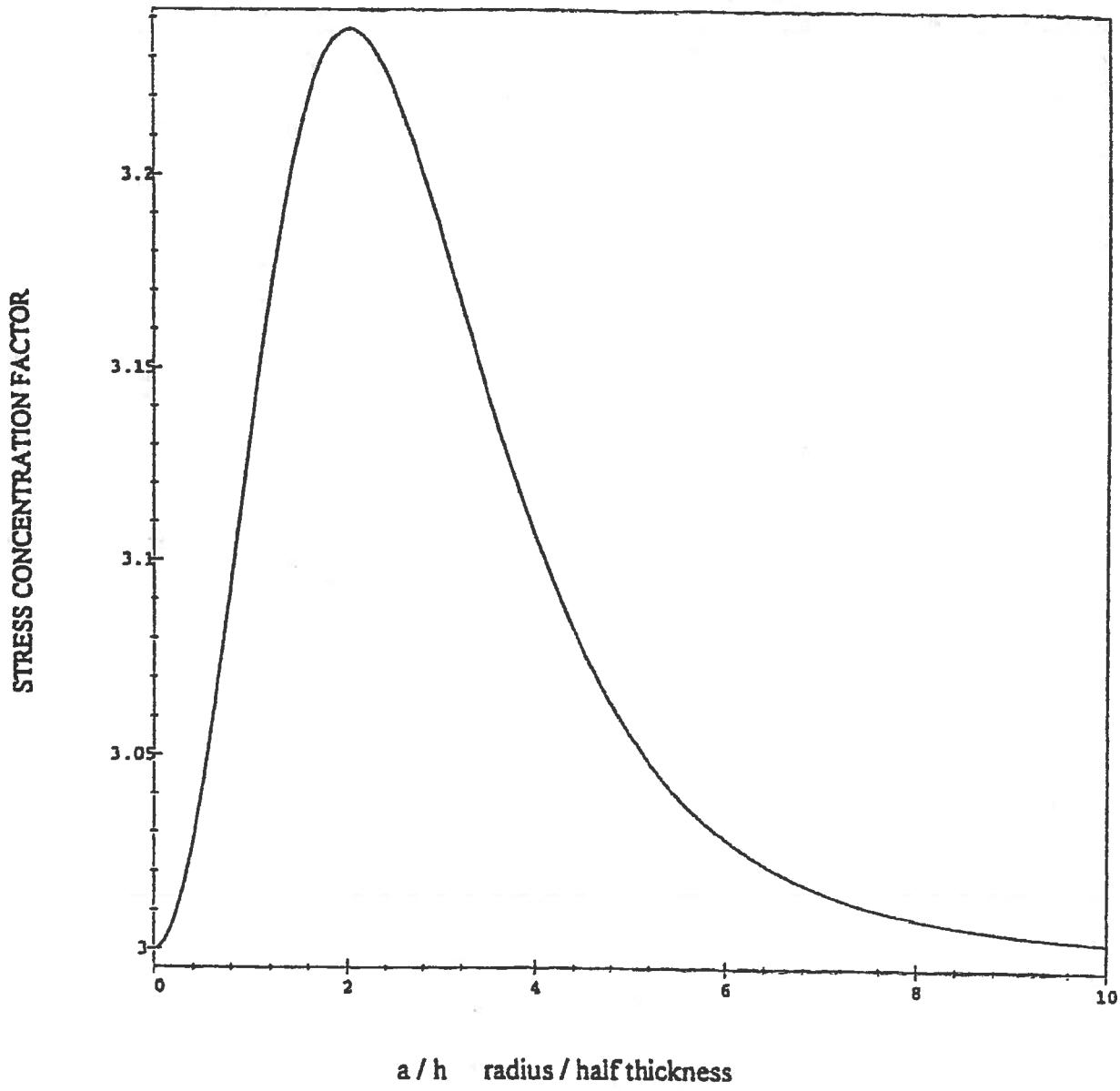


Fig. 1 Maximum stress concentration factor versus radius to half thickness ratio.

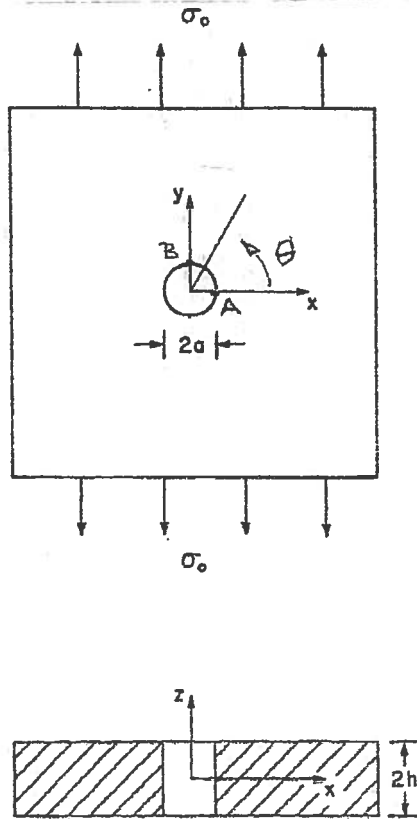


Fig. 2 Infinite plate with a circular hole.

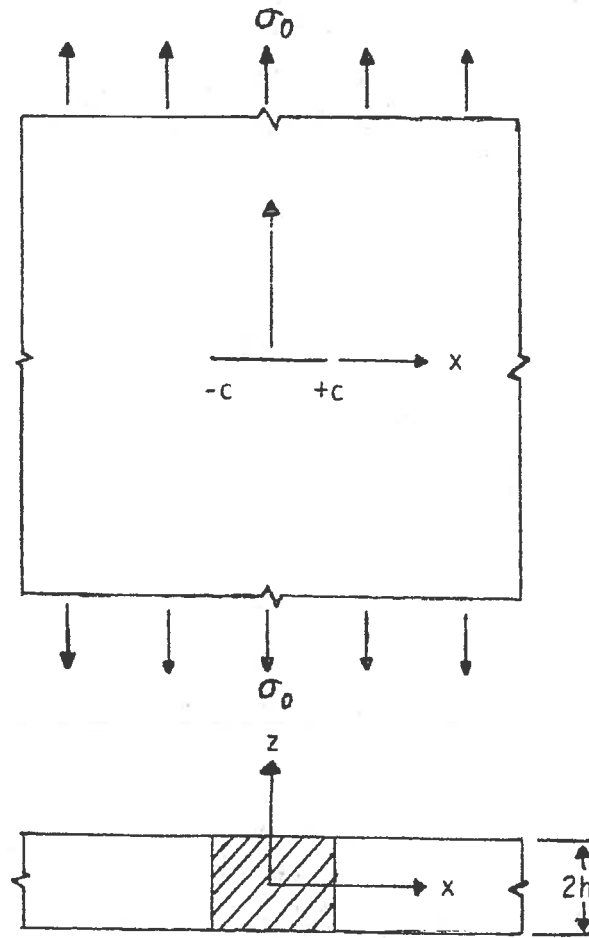


Fig. 3 Infinite plate with a crack.

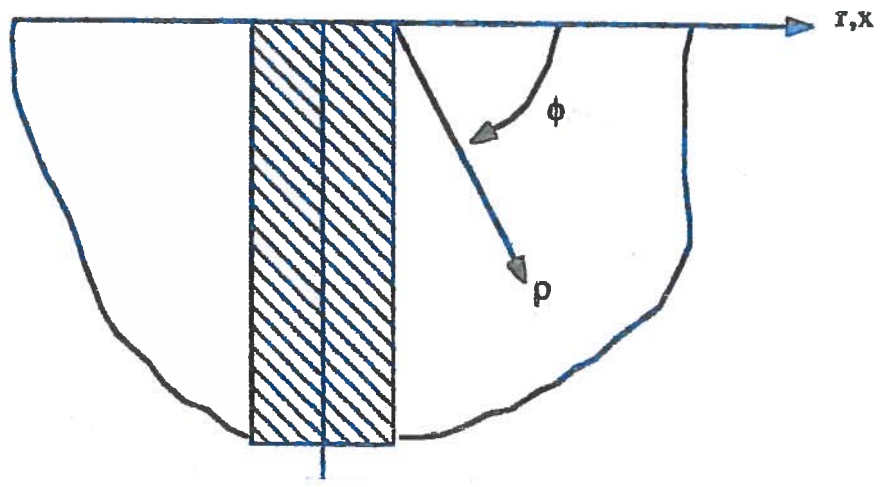


Fig. 4 Local geometry at the corner point.